

Xenon Hydrate Dissociation Measurements With Model Protein Systems

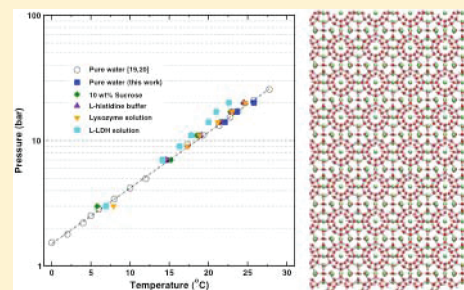
Ryan D. Booker,[†] Carolyn A. Koh,[†] E. Dendy Sloan,[†] Amadeu K. Sum,^{*,†} Evgeniy Shalaev,[‡] and Satish K. Singh[§]

[†]Center for Hydrate Research, Chemical and Biological Engineering Department, Colorado School of Mines, Golden, Colorado 80401, United States

[‡]PharmaTherapeutics Pharmaceutical Sciences, Pfizer Inc., Groton, Connecticut 06340, United States

[§]Biotherapeutics Pharmaceutical Sciences, Pfizer Inc., Chesterfield, Missouri 63017, United States

ABSTRACT: Effective long-term storage remains a significant challenge to the use and development of protein pharmaceuticals. We have investigated the interactions between clathrate hydrates and model protein solutions to determine the effects on hydrate formation. Here, the dissociation curve and equilibrium conditions for xenon clathrate hydrate with model lysozyme and lactate dehydrogenase (LDH) protein solutions have been studied using calorimetry measurements at pressures ranging from 3 to 20 bar. Sucrose in solution was shown to exhibit small inhibition effects on xenon hydrate formation, shifting the dissociation curve and decreasing the conversion of water to hydrate by 15–26%. The addition of L-histidine buffer and lysozyme at low concentrations did not substantially inhibit hydrate formation. However, small shifts in the dissociation curve were demonstrated for solutions containing LDH. The presence of lysozyme and LDH in solution did not significantly alter the conversion of water to hydrate, indicating that these and similar proteins do not substantially affect the extent of xenon gas hydrate formation. Preliminary experiments were performed for LDH solutions to assess the impact of xenon hydrate formation and dissociation on enzymatic activity, with samples stored in hydrate systems showing small decreases in activity.



INTRODUCTION

Many biological and small-molecular-weight pharmaceuticals are unstable in aqueous solutions. To achieve an acceptable shelf life, such products can be either stored as frozen solutions, at or below -20 to -70 °C, or converted into more stable solids by freeze-drying or alternative methods.¹ Frozen storage, in particular, is a common practice for bulk aqueous solutions of protein and vaccine drug substances.^{2,3} However, storage in the frozen state does not guarantee long-term stability. Indeed, aggregation has been reported to occur during long-term storage of bulk proteins in the frozen state.^{4–6} In addition, frozen materials need to be converted to liquids prior to use, which can be time-intensive and usually requires special thawing protocols to minimize loss of activity during the thawing process.⁷ Alternatively, the solution-unstable products, including proteins, vaccines, and small molecules, can be converted into a solid state using, for example, freeze-drying methods. Such dried solids can generally be stored above 0 °C, as seen by the number of commercial biological products that are lyophilized and labeled for storage at 2–8 °C. However, while freeze-drying is a common pharmaceutical process, it is expensive and requires significant capital investments for acquiring and maintaining manufacturing facilities. Processing of large (~ 100 s of liters) quantities of bulk protein solution by freeze-drying is impractical. Therefore, identification of an alternative technology to both freeze storage and freeze-drying is highly desirable.

A potential alternative method for solidifying aqueous solutions is the use of clathrate hydrates. Clathrate hydrates are

water-based crystalline compounds consisting of a lattice-like network of hydrogen-bonded water molecules that form cavities into which small (usually <0.9 nm), nonpolar guest molecules, typically gases, are incorporated. Commonly, clathrate hydrates consist of approximately 85 mol % water and 15 mol % guest(s) molecules.⁸ Most commonly, clathrate hydrates are formed when the guest molecules contact water at elevated pressures and low temperatures.⁹ Examples of clathrate-forming molecules include methane, carbon dioxide, argon, and a number of other small organic and inorganic molecules.^{9–11} One example of a common clathrate hydrate is CO_2 , which can form at approximately 10 MPa and 10 °C.¹² However, high-pressure conditions are not always needed to form clathrates above 0 °C; there are compounds that form clathrate hydrates at atmospheric conditions, such as tetrahydrofuran and cyclopentane, which have dissociation temperatures of 4.4 and 7.7 °C, respectively, at atmospheric pressure.

Practical applications of clathrate hydrates are most extensive in fields related to flow assurance and energy transportation, storage, and recovery.¹³ While there are limited reports on the impact of clathrate hydrates on proteins and other pharmaceutical systems of interests, a select number of studies have provided relevant foundation to the problem herein. One of the first studies of clathrate hydrates in a biorelated area involved

Received: May 13, 2011

Revised: July 13, 2011

Published: July 26, 2011

the stabilization of an enzyme during formation of clathrate hydrates.¹⁴ In a similar study, solidification of some model and food systems in clathrate hydrates at temperatures above 0 °C was shown to significantly inhibit oxidative degradation of ascorbic acid.^{15,16} It is also interesting to note that clathrate hydrates have apparently been applied for the cryopreservation of human skin allografts (for burn management) using xenon and other clathrate-forming gases.¹⁷ However, the interactions of biologically and pharmaceutically relevant proteins with clathrate hydrates remain undercharacterized. In order to investigate potential applications to the stabilization of proteins and other substances of pharmaceutical interest, an initial understanding of the thermodynamics of such a protein–clathrate hydrate system is essential.

Here, we present data on the formation and dissociation of xenon hydrates at a range of pressures and on the hydrate equilibrium conditions in solutions of lysozyme or L-lactic dehydrogenase (L-LDH) with an L-histidine buffer. Lysozyme, a glycoside hydrolase, catalyzes the hydrolysis of β -(1-4)-glucosidic linkages between N-acetylmuramic acid and N-acetyl-D-glucosamine residues in some bacterial cell walls.¹⁸ It is found abundantly in a number of tissues and biological fluids, as well as in chicken egg white. Due to its long-standing use in research, having been first described in 1909,¹⁹ and its well-characterized structure and function,²⁰ lysozyme is well-suited to investigation of the interactions between proteins and clathrate hydrates. L-LDH is another popular model protein used in studies of mechanisms of cryo- and lyo-protection. L-LDH catalyzes the interconversion of pyruvate and lactic acid in an NADH-dependent reaction.²¹ It has been shown to be sensitive to thermal denaturation at temperatures around 50 °C²² and is easily destabilized by freezing and drying.²³

The thermodynamic properties of xenon hydrate, as well as those of many other gas hydrates, have been extensively studied over a wide range of temperatures and pressures.^{24,25} However, little investigation has been done on the interactions between hydrated proteins and clathrate hydrates. Zeng et al. investigated the effects of antifreeze proteins (AFPs) on tetrahydrofuran, propane, and methane clathrate hydrates, finding that AFPs inhibited initial hydrate formation and eliminated the so-called hydrate “memory effect”.^{26–28} Jensen et al. also found inhibitory effects on methane hydrate formation by ice-structuring proteins (ISPs).²⁹ Thus, as previous studies have been limited to AFPs and ISPs and have shown only inhibitory effects of proteins on clathrate hydrate formation, further investigation of the thermodynamic impacts of proteins on clathrate hydrates is necessary to determine if storage of pharmaceutical proteins with hydrates is thermodynamically viable.

The primary objective of this work was to study the formation of clathrate hydrates from model protein solutions, with an ultimate goal of identifying specific conditions (pressure/temperature) to solidify a model protein solution with clathrate hydrates. In addition, a preliminary evaluation of the impact of protein storage in clathrate hydrates on protein stability was made to provide a basis for future examinations of the effects of these crystalline structures on proteins.

MATERIALS AND METHODS

Xenon (Xe) gas (99.999% purity) was obtained from Matheson Tri-Gas. L-Histidine (99% minimum purity), L-histidine monohydrochloride monohydrate (98% minimum purity), lysozyme from chicken egg white (40 000 units/mg of protein minimum activity), and L-lactic dehydrogenase (L-LDH) from rabbit

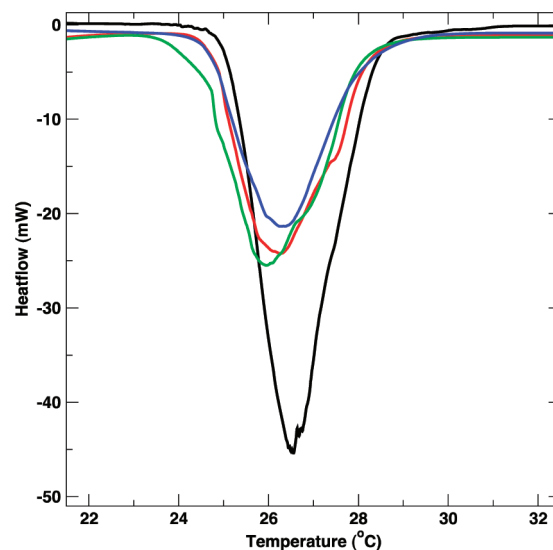


Figure 1. Examples of DSC curves obtained for pure water (black), 10% sucrose (red), sucrose + buffer (green), and lysozyme (blue) solutions with Xe at 20 bar. The onset of the dissociation curve is taken as the hydrate dissociation temperature.

muscle (700–1200 units/mg) were acquired from Sigma-Aldrich. Ultra-pure-grade sucrose was supplied by J.T. Baker.

Four solutions were prepared for use in all experiments, a 10% by weight sucrose solution, a 20 mM L-histidine buffer solution (pH 5.5) with 10% sucrose, a lysozyme solution consisting of 10 mg/mL protein + 10% sucrose + 20 mM histidine buffer at pH 5.5, and an L-LDH solution with 2 mg/mL protein + 10% sucrose + 20 mM histidine buffer at pH 5.5. The buffer solution consisted of sucrose, which is known to stabilize protein structure,³⁰ dissolved in distilled water to 10% by weight, L-histidine dissolved to 0.68 mg/mL, and L-histidine monohydrochloride monohydrate dissolved to 3.27 mg/mL. For the solutions involving protein, either lysozyme or L-LDH was dissolved in the L-histidine buffer solution.

The xenon hydrate dissociation temperatures were measured in a high-pressure microdifferential scanning calorimeter (μ -DSC VIIa, Setaram Inc.) for five different systems, distilled water, 10% sucrose solution, L-histidine buffer solution, 10 mg/mL lysozyme solution, and 2 mg/mL L-LDH solution. Samples of 15–60 mg were placed in a Hastelloy C276 cell with a fixed volume of 0.5 mL. The sample cell and a reference cell were connected to the xenon cylinder through a custom-designed high-pressure panel.³¹ Heating and cooling of the cells were achieved using Peltier heating elements.

The experimental procedure for the measurements in the DSC was as follows. The samples were pressurized at a selected Xe pressure (3–20 bar), cooled at a rate of 5 °C/min from 40 °C for lysozyme and 32 °C for L-LDH to –10 °C, and then held isothermally at –10 °C until an exothermic heat flow peak, indicating hydrate formation, was observed. The temperature was then ramped back to the starting temperature, with a heating rate of 0.5 °C/min maintained through the hydrate dissociation region, with hydrate dissociation indicated by an endothermic heat flow peak. The dissociation temperature was determined as the temperature at which the onset of the endothermic heat flow peak occurred. Figure 1 shows representative endothermic heat flow peaks for four different solutions.

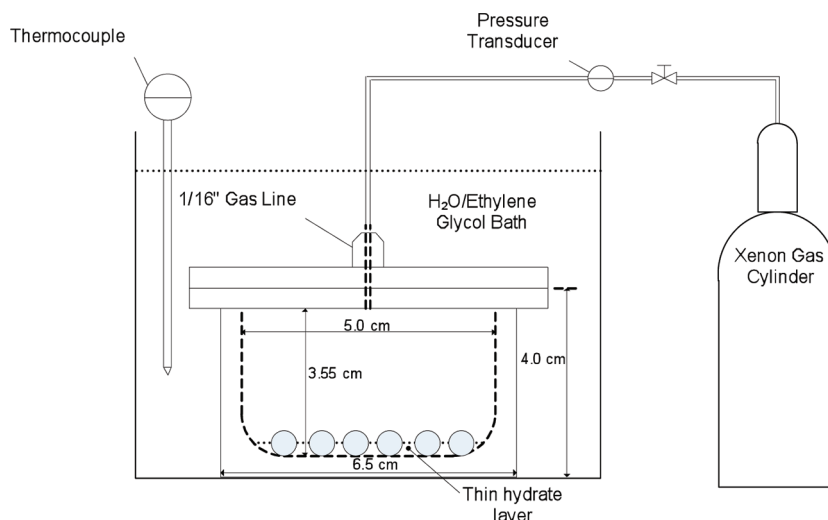


Figure 2. Diagram of the custom stainless steel cell and hydrate formation apparatus (not to scale). The internal volume of the cell is approximately 70 mL. The 1/8 in. diameter stainless steel balls were placed in the cell to improve mixing.

Dissociation temperatures were determined over a range of pressures, from 3 to 20 bar, for each of the five systems. Ice formation did not occur in the experiments performed with Xe. Without Xe at atmospheric pressure, the onset of freezing (ice nucleation) was observed at approximately -17 to -19 °C. Thus, deviations from the heat flow baseline during dissociation temperature measurements are indicative only of hydrate formation and dissociation.

In order to further investigate the thermodynamics of hydrate formation in the model protein solution, experiments were performed in a set of stainless steel cells of in-house design (Pfizer Inc.). The internal volume of each cell was 70 mL. A rubber ring between the body and lid of each cell provided a seal when under pressure, and the lids were modified to add 1/16 in. Swagelok tube fittings for a gas line. The xenon cylinder was connected to the cell through a custom-designed pressure panel with 1/16 in. stainless steel tubing. Heating and cooling were achieved using a Neslab Instruments RTE-110 bath/circulator. Figure 2 shows a schematic of the high-pressure cell and experimental setup for the measurements.

Experiments were conducted with an L-LDH solution in which L-LDH was dissolved to 2 mg/mL in histidine buffer. Samples (5 mL) were placed in the experimental cell, and the system was pressurized with Xe to 20 bar at 30 °C. The temperature was then ramped down to 5 °C and held until a substantial pressure drop was observed, indicating hydrate formation. After completion of hydrate formation, the temperature was ramped up to 30 °C. Experiments were conducted with and without the presence of 1/8 in. stainless steel balls, which were placed in the cell and used for agitation and to increase the interfacial area between the xenon gas and the solution during hydrate formation, in the L-LDH solution. Three samples were used for comparison purposes with the samples stored as hydrates, (i) a sample frozen in liquid nitrogen (frozen), (ii) a sample stored at room temperature (standard), and (iii) a sample subjected to temperatures of ~ 52 °C for 15–20 min (heat denatured). All four samples were stored in their respective conditions for approximately 24 h prior to measurement of enzymatic activity.

The enzyme activity of all four samples was then determined by optical absorbance assay using a kit purchased from the

Biomedical Research Service Center at SUNY—Buffalo. The assay uses the reduction of the tetrazolium salt INT to formazan in an NADH-coupled reaction catalyzed by L-LDH. The reaction produces a red color in solution, which increases with increasing L-LDH activity. The absorbance was measured in a PerkinElmer Victor X5 multilabel plate reader at 490 nm.

RESULTS AND DISCUSSION

Representative DSC curves showing dissociation of hydrate during heating are shown in Figure 1. The smaller secondary peaks observable in the curves for pure water and, to a lesser extent, the 10% sucrose solution may be indicative of a previously unknown phenomenon in the mechanism of xenon hydrate formation, which is being further investigated. However, the phenomenon does not appear to be relevant specifically to the influence or stabilization of proteins or the model protein system used here. The measured xenon hydrate dissociation temperatures for each of the five solutions are summarized in Table 1 and plotted in Figure 3, along with literature data for pure xenon hydrates. To provide a basis for comparison of the dissociation temperatures, the dissociation temperatures for xenon hydrate with pure water over the same range of pressures as for those the other solutions were measured. The dissociation temperatures for the pure water system are in close agreement with published results,^{24,25} differing by an average of 0.49 °C when considering all of the data points measured. A full comparison of these data is shown in Table 1.

The results shown in Table 1 and Figure 3 demonstrate a minimal impact of the presence of sucrose, the histidine buffer, lysozyme, or L-LDH on the xenon hydrate dissociation temperature, which is expected because dissociation temperature is a colligative property that depends on the molar concentration of a solute. At pressures greater than 10 bar, the presence of sucrose decreases the dissociation temperature versus that for xenon hydrate in pure water by approximately 0.8 °C on average, with the shift at the three highest pressures being greater than or very close to the experimental error. At 7 bar, this drop in dissociation temperature was not observed. While the shift in the equilibrium phase coexistence curve shown in Figure 3 is at the outer range of the experimental uncertainty, the consistent decrease and the

Table 1. Measured Dissociation Temperatures for Xenon Hydrate^a

pressure (bar)	hydrate dissociation temperature (°C)				
	water	10% sucrose	histidine buffer	lysozyme solution	L-LDH solution
3		5.8		7.9	6.9
7	14.6	15.2	14.6	14.3	14.1
9				17.4	16.3
11	18.9	18.5	17.8	18.9	17.8
14	22.1	21.4	21.7	21.2	20.0
17	23.6	22.8	23.0	23.0	21.0
20	25.8	24.5	24.5	24.7	22.6

^a The estimated error in the measurements is $\pm 0.43^\circ\text{C}$. The 10 wt % sucrose solution is prepared in DI water. The histidine buffer solution is a solution of 20 mM L-histidine buffer (pH 5.5), consisting of 10 wt % sucrose, 0.68 mg/mL L-histidine, and 3.27 mg/mL L-histidine monohydrochloride monohydrate, dissolved in DI water. The lysozyme solution consists of 10 mg/mL lysozyme dissolved in the histidine buffer solution. The L-LDH solution consists of 2 mg/mL L-LDH dissolved in the histidine buffer solution.

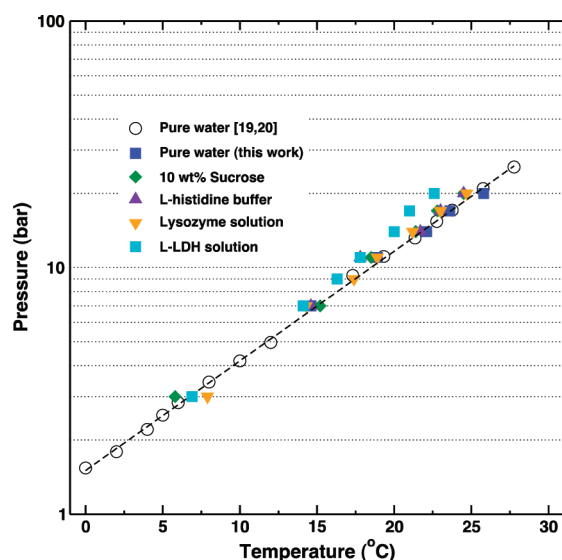


Figure 3. Dissociation curves for xenon hydrate for five experimental solutions listed in Table 1, water only, 10 wt % sucrose, histidine buffer solution, lysozyme solution, and L-LDH solution.

substantial decrease in the extent of water converted to hydrate discussed below indicate a small inhibition effect of sucrose on hydrate formation. However, no significant additional inhibition effects are observed due to the presence of the histidine buffer or lysozyme in solution. Of particular significance is the lack of effect of the presence of lysozyme in solution on the hydrate dissociation temperature. At a given pressure, the difference in dissociation temperature between the hydrate formed in pure water and the hydrate formed in lysozyme solution is never greater than 1.1°C , within the range of experimental error at all temperatures, except at 20 bar, and the average temperature difference is 0.55°C . The unaltered dissociation temperatures suggest that the mechanism and thermodynamics of xenon gas hydrate formation are not substantially affected by the presence of lysozyme in solution.

The presence of L-LDH, unlike that of lysozyme, shows a small effect beyond that caused by the sucrose, decreasing the hydrate dissociation temperature by an average of 1.9°C , an additional 1.1°C beyond the average decrease caused by sucrose, from the dissociation temperature in pure water at

the pressures measured. This result is unexpected given that the low concentrations of LDH, corresponding to approximately 14.3 mM, should be too small to produce a substantial shift in the hydrate dissociation temperature. It is likely that this shift is due to nonequilibrium effects arising from the fact that the concentration of LDH in the “hydrate-concentrated” solution shifts during the course of the dissociation temperature measurement. Thus, as hydrate formation progresses, the concentration of sucrose and L-LDH in the water that remains available for conversion to hydrate increases, shifting the hydrate dissociation temperature downward. In addition to the shift in the dissociation temperature, the L-LDH solution also produced a small change in the slope of the dissociation curve. Such an increase in slope indicates a change in the heat of dissociation, but the potential mechanism of such a shift is unclear and requires further investigations.

For protein stabilization, a critical parameter is the extent of water-to-hydrate formation. Indeed, a necessary, although not sufficient, condition for long-term stability is converting the protein-containing phase into a glassy state by removal of water in the form of clathrate hydrate and increasing the glass transition temperature (T_g) of the protein-containing phase to above the storage temperature. Therefore, it is essential to devise a method to estimate the extent of water-to-hydrate formation. In DSC experiments, the enthalpy of hydrate dissociation can be used to estimate the extent of conversion. On the basis of the experimentally determined hydrate dissociation enthalpies, the percentages of water converted to hydrate for each of the five experimental systems were determined at 7, 14, and 20 bar, as well as at four other pressures for the protein systems. The amount of water converted to hydrates is shown in Table 2. These were calculated based on the heat evolved from the samples measured in the dissociation part of the measurements. The heat of dissociation for the hydrates used in calculations was -15.5 kcal/mol .³²

As indicated by the shifts in the phase coexistence curves, sucrose appears to exert a small inhibitory effect on xenon hydrate formation. Here, the presence of sucrose causes a decrease of 15–26% in the percentage of water converted to hydrate during the hydrate formation process. These decreases are likely due to kinetic factors and exclusion of water from the hydrate nucleation region. The formation of hydration shells around sucrose molecules decreases the water available for clathrate hydrate nucleation at the water–xenon hydrate interface.

Table 2. Conversion of Water to Xenon Hydrate in DSC Measurements^a

pressure (bar)	percentage conversion of water to hydrate				
	water	10 wt % sucrose	histidine buffer	lysozyme solution	L-LDH solution
3				36.4%	41.0%
7	66.4 ± 0.8%	55.9 ± 2.9%	68.2 ± 5.8%	61.2 ± 9.1%	66.1 ± 8.2%
9				57.9%	52.0%
11				58.8%	54.5%
14	63.5 ± 10.3%	45.5 ± 0.6%	51.0 ± 0.1%	58.5 ± 1.4%	65.2 ± 8.1%
17				36.5%	62.9%
20	64.6 ± 2.5%	47.8 ± 0.8%	52.5 ± 0.1%	45.0 ± 5.0%	64.1 ± 5.2%

^a Error values are the standard deviation for two measurements.

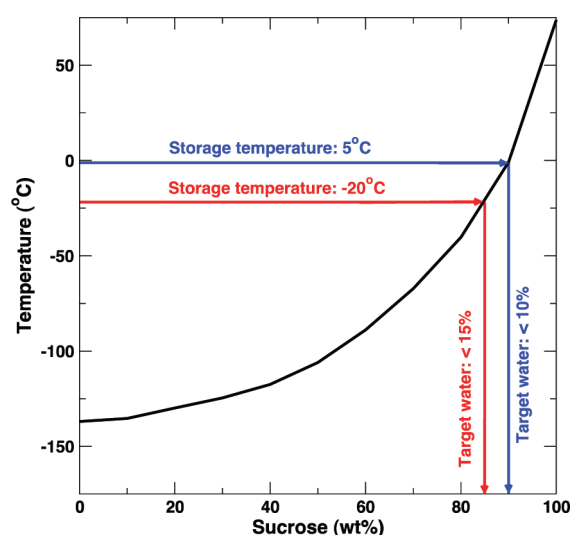


Figure 4. Glass transition temperature (T_g) for the sucrose–water system.

The addition of the histidine buffer and the two proteins, however, does not cause any additional decreases in conversion to hydrate. In fact, the conversion to hydrate is slightly greater for the L-LDH solution than for the sucrose solution. However, due to the uncertainty in this measurement and the downward shift in the hydrate dissociation curve for the L-LDH solution, it can only be concluded that L-LDH does not decrease the extent of conversion to hydrate.

As shown in Table 2, only approximately 50% of water is removed from the solution as a clathrate hydrate. In order to convert the “hydrate-concentrated solution” (which contains all of the solutes and remaining water) to the glassy state at the desired temperature, a much higher extent of conversion is required. To provide a more quantitative estimation of the target extent of conversion, it is convenient to look at the water–sucrose system, for which the T_g at different concentrations is well-documented.³³ The T_g is presented in Figure 4 as a function of water content. As shown in Figure 4, the target water content in the hydrate-concentrated solution (assuming that Xe has a minimal effect on the T_g) depends on the storage temperature. For example, if the storage temperature is $-20\text{ }^{\circ}\text{C}$, the water content should be less than 15 wt % (i.e., sucrose concentration more than 85 wt %) to ensure sucrose in the amorphous solid (glassy) state. To achieve this low water content by hydrate formation, the extent of water-to-

hydrate conversion should be at least 95%. It is obvious from Table 2 that the extent of the conversion is insufficiently high to convert the hydrate-concentrated solution to the glassy state at reasonably high temperatures. The relatively low percentages of water converted to hydrate, shown in Table 2, indicate that hydrate conversion is occurring only at the gas–liquid interface. Increased conversion of the solution to hydrate can likely be achieved through improved mixing, but this cannot be controlled in the calorimetry apparatus used here.

In a separate set of experiments, the impact of hydrate formation on the activity of L-LDH was studied using a specially designed cell (Figure 2). In these experiments, the formation of hydrate was determined from the pressure drop, as shown in Figure 5.

Preliminary results for the L-LDH activity are shown in Figure 6. These results indicate that only a small decrease in L-LDH activity occurs during the hydrate conversion process, dropping an average of 11.5% from the sample stored at room temperature. Furthermore, less loss of activity is observed for the samples in which the hydrate was formed than in the samples that were frozen. Note that freeze-induced destabilization of proteins is usually related to destabilization by ice crystals, either via sorption of proteins on the ice/solution interface³⁴ or mechanical stresses due to volume expansion as a result of the water-to-ice transformation.³⁵ Alternatively, low temperature per se may lead to protein unfolding (so-called cold denaturation),^{36,37} although this process is often reversible. For L-LDH, the cold denaturation temperature was reported to be $-28\text{ }^{\circ}\text{C}$, although the presence of different solutes can impact both the thermodynamics and kinetics of cold denaturation.³⁸ Therefore, loss of protein activity observed with clathrate hydrates may be caused by either protein sorption on the hydrate/solution interface or mechanical stresses due to hydrate crystal growth, by analogy with freezing processes. Lower loss of protein activity observed with hydrates (and therefore better stability of protein with hydrates as compared to freezing) may be because protein exposure to low temperatures (and therefore cold denaturation) has been avoided in clathrate hydrate samples. However, further study is needed to elucidate the destabilization mechanisms associated with clathrate hydrates. For comparison purposes, a sample that should show partial heat denaturation was included in the L-LDH activity assays. It should be noted that these results are preliminary, and further experiments are required to verify and fully characterize the effects of the hydrate formation process on the model protein solution. These will be presented in a future publication.

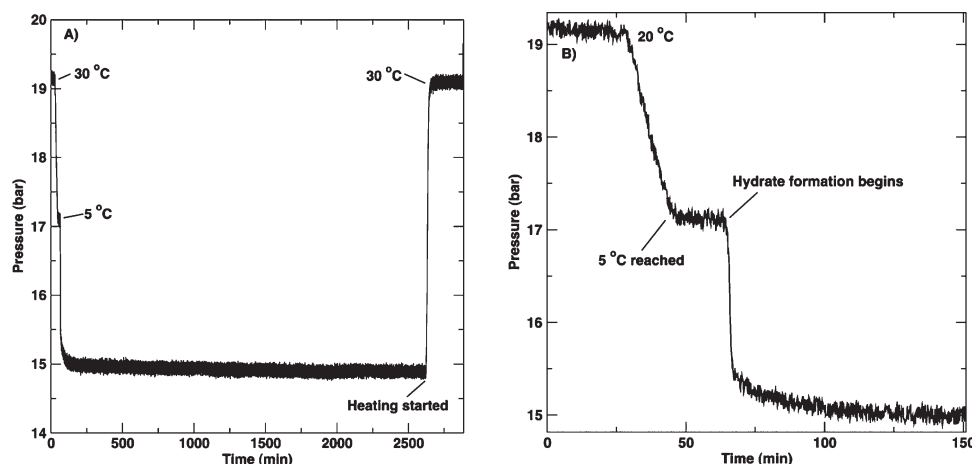


Figure 5. Pressure trace in the pressure cell during (A) an entire hydrate formation and dissociation cycle and (B) the hydrate formation process. At 19.1 bar, the hydrate equilibrium temperature is 22.9 °C.

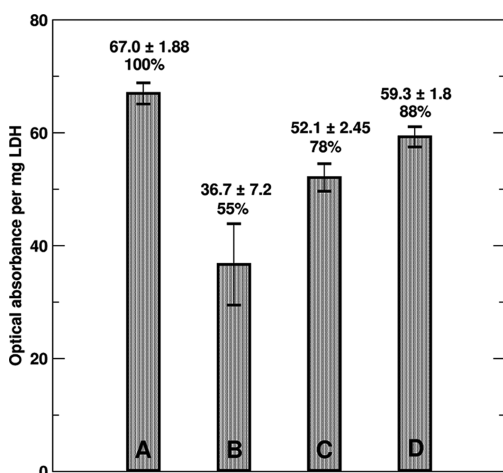


Figure 6. Average optical absorbance per mg of L-LDH in original solutions at 490 nm for (A) standard L-LDH samples that were stored at room temperature, (B) heat-denatured samples, (C) samples frozen in liquid nitrogen, and (D) samples stored as hydrates. Averages are for four independent trials. The basis for percentages is the standard sample as 100%.

CONCLUSIONS

Calorimetric data has been used to determine the dissociation curve for xenon hydrate with model protein systems over a range of pressures from 3 to 20 bar. The presence of sucrose in solution exerted small inhibition effects on the formation of xenon hydrate, decreasing the dissociation temperature by an average of 0.8 °C and decreasing conversion of water to hydrate by 15–26%. Further addition of a histidine buffer and lysozyme did not produce significant additional inhibition, indicating that lysozyme and similar proteins do not significantly alter or inhibit the mechanism of xenon clathrate hydrate formation. The addition of L-LDH did produce a shift in the dissociation curve, decreasing the dissociation temperatures by an average of 1.9 °C. However, no decrease in the extent of conversion to hydrate was observed. It is likely that the shift in dissociation temperature occurs due to nonequilibrium effects during the dissociation measurement, but further study is needed. Thus, while previous data have shown inhibitory effects of antifreeze proteins and

ice-structuring proteins on clathrate hydrate formation, the data presented here indicate no substantial inhibition of the extent of hydrate formation by more pharmaceutically representative proteins such as lysozyme and L-LDH. Furthermore, preliminary measurements suggest that there is potential merit in using clathrate hydrates for the preservation of proteins, as measured by the activity of L-LDH in solution before and after hydrate formation.

AUTHOR INFORMATION

Corresponding Author

*E-mail: asum@mines.edu.

ACKNOWLEDGMENT

This work was financially supported by Pfizer Inc. and partially supported by the National Science Foundation under Grant No. 0828649. A.K.S. acknowledges the support of DuPont for a DuPont Young Professor Award. The authors thank Prof. Keith B. Neeves and Abimbola Onasoga for use of the multilabel plate reader for the protein assay and Drs. Dirk Teagarden and Phil Nixon for encouraging that this investigation be performed.

REFERENCES

- (1) Wang, W. *Int. J. Pharm.* **2000**, *203*, 1–60.
- (2) Singh, S.; Kolhe, P.; Wang, W.; Nema, S. *Bioprocess Int.* **2009**, *7*, 32–44.
- (3) Singh, S.; Kolhe, P.; Wang, W.; Nema, S. *Bioprocess Int.* **2009**, *7*, 34–42.
- (4) Privalov, P. L. *Crit. Rev. Biochem. Mol. Biol.* **1990**, *25*, 281–305.
- (5) Piedmonte, D. M.; Summers, C.; McAuley, A.; Karamujic, L.; Ratnaswamy, G. *Pharm. Res.* **2007**, *24*, 136–146.
- (6) Singh, S.; Kolhe, P.; Mehta, A.; Chico, S.; Lary, A.; Huang, M. *Pharm. Res.* **2011**, *28*, 873–884.
- (7) Cao, E.; Chen, Y.; Cui, Z.; Foster, P. *Biotechnol. Bioeng.* **2003**, *82*, 684–690.
- (8) Sloan, E. D. *Ind. Eng. Chem. Res.* **2000**, *39*, 3123–3129.
- (9) Sloan, E. D.; Koh, C. A. *Clathrate Hydrates of Natural Gases*, 3rd ed.; CRC Press: Boca Raton, FL, 2008.
- (10) Englezos, P. *Ind. Eng. Chem. Res.* **1993**, *32*, 1251–1274.
- (11) Werezak, G. N. *Chem. Eng. Prog. Symp.* **1969**, *65* (91), 6–18.
- (12) Someya, S.; Bando, S.; Chen, B.; Song, Y.; Nishio, M. *Int. J. Heat Mass Transfer* **2005**, *48*, 2503–2507.

- (13) Sum, A. K.; Koh, C. A.; Sloan, E. D. *Ind. Eng. Chem. Res.* **2009**, *48*, 7457–7465.
- (14) Lund, D.; Fennema, O. *Arch. Biochem. Biophys.* **1969**, *129*, 181–188.
- (15) Thompson, L. U.; Fennema, O. *J. Food Sci.* **1970**, *35*, 640–641.
- (16) Thompson, L. U.; Fennema, O. *J. Agric. Food Chem.* **1971**, *19*, 232–235.
- (17) IBPT Corporation. *I B P T Corporation*. <http://ibpt.cryostasis.com/> (accessed Dec 22, 2010).
- (18) Cates, S. *Expasy Proteomics Tools, Connexions Web site*. <http://cnx.org/content/m11082/2.5/> (accessed Dec 22, 2010).
- (19) Laschtschenko, P. Z. *Hyg. Infektionskrankh.* **1909**, *64*, 419–427.
- (20) Merlini, G.; Bellotti, V. *Clin. Chim. Acta* **2005**, *357*, 168–172.
- (21) Holbrook, J. J.; Liljas, A.; Steindel, S. J.; Rossman, M. D. *Lactate Dehydrogenase*. In *The Enzymes*; Academic Press: New York, 1975.
- (22) Hochachka, P. W. *Comp. Biochem. Physiol.* **1968**, *27*, 609–611.
- (23) Chatterjee, K.; Shalaev, E. *Pharm. Res.* **2005**, *22*, 303–309.
- (24) Ohgaki, K.; Sugahara, T.; Suzuki, M.; Jindai, H. *Fluid Phase Equilib.* **2000**, *175*, 1–6.
- (25) Dyadin, Y.; Larionov, E. G.; Mirinskij, D. S.; Mikina, T. V.; Aladko, E.; Starostina, L. I. *J. Inclusion Phenom. Macrocycl. Chem.* **1997**, *28*, 271–285.
- (26) Zeng, H.; Wilson, L.; Walker, V. *Can. J. Phys.* **2003**, *81*, 17–24.
- (27) Zeng, H.; Moudrakovski, I. L.; Ripmeester, J. A.; Walker, V. K. *AIChE J.* **2006**, *52*, 3304–3309.
- (28) Zeng, H.; Wilson, L. D.; Walker, V. K.; Ripmeester, J. A. *J. Am. Chem. Soc.* **2006**, *128*, 2844–50.
- (29) Jensen, L.; Ramlov, H.; Thomsen, K.; von Solms, N. *Ind. Eng. Chem. Res.* **2010**, *49*, 1486–1492.
- (30) Lee, J.; Timasheff, S. J. *Biol. Chem.* **1981**, *256*, 7193–7201.
- (31) Lachance, J. W. *Investigation of Gas Hydrates Using Differential Scanning Calorimetry with Water-in-Oil Emulsions*. Masters Thesis, Colorado School of Mines, Golden, CO, 2008.
- (32) Ewing, G. J.; Ionescu, L. G. *J. Chem. Eng. Data* **1974**, *19*, 367–369.
- (33) Girlich, D.; Lüdemann, H. D. *Z. Naturforsch.* **1994**, *49*, 250–257.
- (34) Strambini, G.; Gonnelli, M. *Biophys. J.* **2007**, *92*, 2131–2138.
- (35) Varshney, D.; Elliott, J.; Gatlin, L.; Kumar, S.; Suryanarayanan, R.; Shalaev, E. *J. Phys. Chem. B* **2009**, *113*, 6177–6182.
- (36) Franks, F.; Hatley, R.; Friedman, H. *Biophys. Chem.* **1988**, *31*, 307–315.
- (37) Tang, X.; Pikal, M. *Pharm. Res.* **2005**, *22*, 1167–1175.
- (38) Hatley, R.; Franks, F. *FEBS Lett.* **1989**, *257*, 171–173.